

## **Aerodynamics of Ground Mounted Solar Panels: Test Model Scale Effects**

Aly Mousaad ALY<sup>1)</sup> and Girma BITSUAMLAK<sup>2)</sup>

<sup>1</sup> *Research Fellow, WindEEE Research Institute, Department of Civil and Environmental Engineering, Western University, Boundary Layer Wind Tunnel Laboratory, London, ON, Canada, N6A 5B9, [aalysaye@UWO.ca](mailto:aalysaye@UWO.ca)*

<sup>2</sup> *Associate Professor, Associate Director WindEEE Research Institute, Department of Civil and Environmental Engineering, Western University, Boundary Layer Wind Tunnel Laboratory Rm. 105, London, ON, Canada, N6A 5B9, [gbitsuam@UWO.ca](mailto:gbitsuam@UWO.ca)*

### **Abstract**

Most boundary layer wind tunnels were built for testing models of large civil engineering structures that have geometric scales ranging from 1:500 to 1:100. However, producing typical aerodynamic models of the solar panel modules at such scales makes the modules too small, resulting into at least two technical problems: first, the resolution of pressure data on such small-scale models becomes low, and second, the test model may be placed in a portion of the boundary layer that might not be a true representative of the boundary layer in real world due to high uncertainty in the wind velocity. To alleviate these problems, standardized testing protocol that accounts for different time and geometric scales is important for designing appropriate wind tunnel experiments that can allow for accurate assessment of the wind loads on the solar panels. The current paper investigates systematically the sensitivity of testing these types of structures in different wind profiles with different integral length scales and different model sizes, with the objective of producing a recommendation on the most practical approach for testing the solar panels. This may lead to a standardized wind tunnel testing procedure for estimating wind loads on small size structures in general and solar panels in particular.

## 1. Introduction

Boundary layer wind tunnel (BLWTL) testing of structures is an industry wide accepted procedure and is considered the main source of information for wind loads calculation and codification. Nevertheless, the majority of the boundary layer wind tunnels are built for testing large civil structure models that have a scale ranging from 1:500 up to 1:100. On the other hand, producing representative aerodynamic models of ground mounted solar panel modules at such scales makes the modules too small, resulting into at least two technical problems: first, the resolution of pressure data on such small models becomes low, and second, the model may lay in a portion of the boundary layer in the tunnel that might not be a representative of the boundary layer in real world. For example, small ground-mounted solar panels, when scaled down, may have a height that is even less than the smallest roughness element (block size) in the upstream wind. Consequently, standardized modeling procedure that accounts for different time and spatial scales is important for designing appropriate wind tunnel experiments to determine the wind loads accurately on the solar panels.

Because of the lack of full-scale data, wind tunnel modeling of solar panels is not often calibrated/validated with the prototype data. Therefore, the scale effects are not well quantified yet. It is clear that a wind tunnel boundary layer should exhibit similar velocity and turbulence intensity profiles as those of the atmospheric boundary layer. What is not well understood is how to select the model scale ratios to minimize the scale effects. According to Zhao et al. (1996) pressure distribution on a bluff body in wind, as long as the roughness height is correctly modeled, correct results of the pressure coefficient on the building surface can be obtained even if the scale ratio of the body size is not

correctly selected. According to Richards et al. (2007), at relatively large-scale wind-tunnel modeling of civil engineering structures, it is very difficult to model the full turbulence spectra and so only the high-frequency end of the spectrum is matched. Bienkewicz et al. (2007) carried out a comparative study of approach flow and wind pressures on low buildings using wind tunnel data generated at six wind engineering laboratories and investigated the variability in the laboratory wind loading. This variability was primarily attributed to differences in the approach flows employed in physical modeling of wind pressures on tested buildings. According to Bienkewicz et al., (2007) the variability in the data collected on low-rise buildings from different six wind tunnels was primarily attributed to differences in the approach flows employed in physical modeling of wind pressures on tested buildings, carried out by the participating laboratories. The variability in the approach flows resulted in a large measure from the differences in the along wind turbulence intensity implied by different empirical models, defining the target wind exposures and used by the laboratories. This indicates the sensitivity of the aerodynamic data to accurate inflow characteristics. This is further complicated when dealing with a scale different from the typical scales where BLWTL are designed for.

The current paper investigates systematically the sensitivity of the aerodynamic data when testing these types of structures at different test model sizes, in different wind profiles with different integral length scales, with the objective of producing a recommendation on the most practical approach for boundary layer wind tunnel testing of the solar panels in particular and small structures in general.

## 2. Methodology

*Solar panel modules:* Four sizes of solar panels are considered in the present boundary layer wind tunnel study, scaled 1:50, 1:20, 1:10 and 1:5 (1:30 is in progress). The tap layout on upper and bottom surfaces of the solar panel modules is shown in Fig. 1. In the figure, hollow circles designate locations of upper and bottom pressure taps and solid circles designate centers of the tributary areas. Tributary boundaries are indicated by thin lines.

Fig. 2 shows instrumented model-scale of a ground-mounted solar panel in the boundary layer test section. Four different arrangements of the modules were tested. The arrangements are: (1) tilt angle  $\alpha$  of  $25^\circ$  and leg height (H) of 24 inches (25degH24), (2) tilt angle of  $25^\circ$  and leg height of 32 inches (25degH32), (3) tilt angle of  $40^\circ$  and leg height of 24 inches (40degH24), and (4) tilt angle of  $40^\circ$  and leg height of 32 inches (40degH32). 1 inch = 0.0254 m. The effect of model scale was studied by considering two modules with different scales (1:20 and 1:10).

*Wind profile.* Four wind profiles were considered in the current study (Fig. 3):

- (1) Low turbulent flow (E0): this profile has less turbulent content at low frequency.
- (2) Open terrain scaled 1:400 (E3): This flow represents the available wind flow that entails to simulating the atmospheric flows of open terrain exposures in a wind flow that is designed for testing models of length scales about 1:400. Such scales are widely used in many boundary layer wind tunnel testing facilities.
- (3) Open terrain scaled 1:20 (E5): This flow was achieved by adjusting the roughness elements at the wind tunnel to increase the turbulence and the

integral length scale and hence producing a wind flow that is simulating open terrain flow scaled 1:20.

(4) High turbulent flow (E7): This flow was achieved by adjusting the roughness elements at the wind tunnel to further increase the turbulence.

The mean wind speed, turbulence intensity and integral length scales of the along wind velocity component are shown in Fig. 3. The generated wind spectrum for the along-wind velocity component is plotted in Fig. 4 in comparison with the von Karaman spectra taken from the literature (Holmes, 2001). Wind pressure data over the upper and bottom surfaces of the modules instrumented in Fig. 2 are collected for time periods of 60 s, 120 s, 240 s and 480 s for modules scaled 1:50, 1:20, 1:10 and 1:5, respectively. The data were collected at a sampling rate of 400Hz.

*Pressure coefficients:* At the location of each pressure tap, the time history of the pressure coefficient,  $C_p(t)$ , is obtained from the time history of the measured differential pressure,  $p(t)$ , as

$$C_p(t) = \frac{p(t)}{\frac{1}{2}\rho U^2} \quad (1)$$

where  $\rho$  is the air density at the time of the test and  $U_{3s}$  is the mean wind speed measured at the mean height of the solar panel..

In designing the solar panels, it is necessary to determine the net pressure on the individual modules. The net pressure coefficient at any location,  $C_{p_{net}}(t)$ , is the simultaneous difference between the upper pressure coefficient at the upper surface,

$Cp_{upper}(t)$ , and the pressure coefficient at the bottom surface,  $Cp_{bot}(t)$ , at the same locations

$$Cp_{net}(t) = Cp_{upper}(t) - Cp_{bot}(t). \quad (2)$$

The coefficient of the normal load acting on test model is defined as follows:

$$CF(t) = \frac{\sum_{i=1}^n Cp_{net,i}(t) \times A_i}{\sum_{i=1}^n A_i} \quad (3)$$

where  $A_i$  is the tributary area of tap number  $i$ ,  $i = 1, 2, 3, \dots, n$  (total number of taps). The maximum (peak) pressure and force coefficient values ( $Cp_{max}$  and  $CF_{peak}$ ) may be obtained from the measured pressure time histories. Nevertheless, these observed peaks can exhibit wide variability from one realization to another due to the highly fluctuating nature of wind pressures. This means that significant differences might be expected in the peak values of pressure time series obtained from several different tests under nominally identical conditions. Therefore it is generally preferable to use a more stable estimator for the expected peaks. To remove the uncertainties inherent in the randomness of the peaks, probabilistic analyses were performed using an automated procedure developed by Sadek and Simiu (2002) for obtaining statistics of pressure peaks from observed pressure time histories. Because estimates obtained from this approach are based on the entire information contained in the time series, they are more stable than estimates based on observed peaks (Aly et al., 2012).

### 3. Results and discussions

Figures 5-10 show mean, root mean square and maximum net pressure coefficients' distribution over model scale solar panels (1:20 and 1:10) under open country exposure "E3." It is shown that both large (1:10) and medium (1:20) models have similar mean pressure distribution. This indicates that the mean pressures are not significantly affected by the model size. On the other hand, both root mean square and maximum pressure coefficient for the medium model (1:20) are higher than those of the larger model (1:10). This reveals the effect of the model size on the fluctuating pressures on ground mounted solar panels. The higher pressure fluctuations on medium size panel are attributed to its location in the boundary layer as the turbulence intensity is higher close to the ground. This means that under the same wind exposure, smaller ground mounted solar panel modules can be immersed in higher turbulent flow while larger modules are located in less turbulent flow.

Fig. 11 shows mean, root mean square and peak normal force coefficients for solar panel modules with tilt angle  $\alpha$  of  $40^\circ$  and leg height (H) of 24 inches (40degH24, see Fig. 2) under different wind exposures. It is shown that the mean values of the normal load coefficients are not significantly affected by the model size (small, 1:50; medium, (1:20); large, 1:10) under four different wind flows. However, for a very large module (scale 1:5), the mean value is slightly higher as this module has a high blockage ratio (7.8 % as shown in Table 1) It is worth noting that all of the wind flows used here have similar high frequency content (see Fig. 4a). This reveals that the mean wind loads on the solar panels remains unchanged regardless of the turbulence intensity and the model size under wind flows that has similar high frequency turbulent. This could be explained by the fact that high frequency turbulence is the key factor that controls the

flow patterns around bluff bodies in general. On the other hand, root mean square and peak wind loads are governed by both the turbulence intensity and as well as the low frequency turbulent. As smaller models are located closer to the ground and hence immersed in a higher turbulent flows, they have higher fluctuating pressures. Flows with higher low frequency turbulence causes higher pressure fluctuation on the solar panels indicated by higher root mean square and maximum load coefficients.

Fig. 12 shows mean, root mean square and peak normal force coefficients for solar panel modules for a total of four configurations: 25degH24, 25degH32, 40degH24 and 40degH32 (see Fig. 2) under open country exposure "E3." It is shown that mean wind loads on very small modules (1:50) can be erroneous as their location very close to the ground where the uncertainty in the wind speed is very high (Fig. 12a, configurations 25degH24 and 25degH32). For large and medium size modules, the wind loads are not significantly affected by changing the leg height 33%.

#### **4. Conclusions**

The paper presents an ongoing wind effect investigation on ground-mounted solar panels with an aim to understand the model scale effects on the pressure distribution and the net loads. The net pressure distribution for ground mounted solar panels, considered in the present study, is significantly dependent on the module scale and the wind exposure. The aerodynamic normal force for the ground-mounted solar panels is highly dependent on the model scale and the flow characteristics. The main contributions of the current study are summarized as follows:



1. Under the same turbulent wind profile, small ground mounted solar panels are located in the lower part of the boundary layer and that is why they have higher root mean square and peak pressures rather than larger models.
2. The mean pressure loads are not significantly affected by turbulence. However, very small size solar panels may have different mean wind loads as they are located very close to the ground and hence, the uncertainty in the aerodynamic data is relatively high.
3. Under very low turbulent wind flow, both large and small size test models have very similar mean pressure loads. However, root mean square and peak loads are slightly different.
4. It might be the turbulence intensity rather than the model size that affects more the wind loadings on the solar panel modules.

## References

- Aly, A.M., Bitsuamlak, G. and Gan Chowdhury, A., (2012), "Full-scale aerodynamic testing of a loose concrete roof paver system," *Engineering Structures* (in press).
- Holmes, D.J. (2001), *Wind Loading of Structures*, Spon Press, London.
- Richards, P.J., Hoxey, R.P., Connell, B.D. and Lander, D.P. (2007), "Wind-tunnel modelling of the Silsoe Cube", *J. Wind Eng. Ind. Aerodyn.*, **95**(9-11), 1384-1399.
- Bienkiewicz, B., J.A. Main, W.A. Fritz, M. Endo. (2007), "Comparative Inter-Laboratory Study of Wind Loading on Low Industrial Buildings," *Wind and Seismic Effects. U.S./Japan Natural Resources Development Program (UJNR). Joint Meeting, 39th. Technical Memorandum of PWRI 4075. Proceedings, Tsukuba, Japan, pp. 409-417.*

Simiu, E. (2009) *Toward a standard on the wind tunnel method*, NIST Technical Note 1655.

Zhao, Y.W., Plate, E.J., Rau, M. and Keiser, R. (1996), "Scale effects in wind tunnel modelling", *J. Wind Eng. Ind. Aerodyn.*, **61**(2-3), 113-130.

## **Tables**

Table 1 Model sizes and the corresponding tunnel blockage ratio

Scale	1 to 5	1 to 10	1 to 20	1 to 50
Blockage (%)	7.88	1.97	0.49	0.03

## Figures

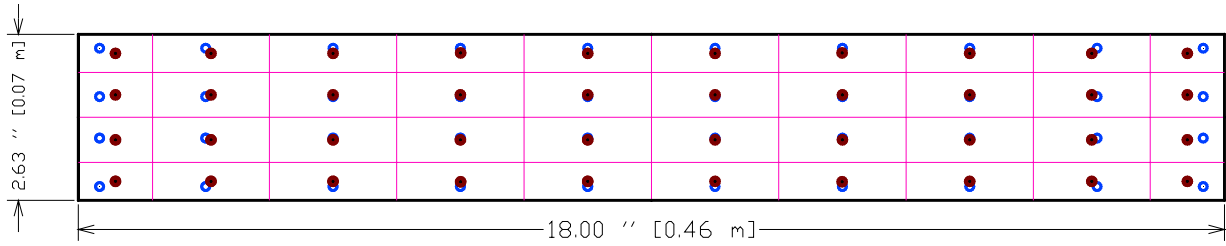


Fig. 1 Tap layout and tributary areas for model-scale (1:20). Hollow circles designate locations of external and underneath pressure taps; solid circles indicate centers of the tributary areas. Tributary boundaries are indicated by thin lines.

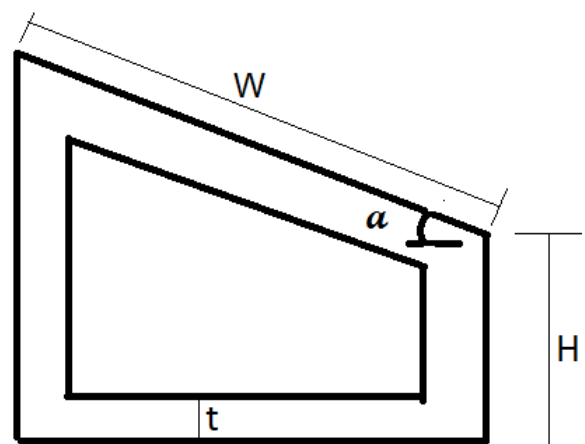
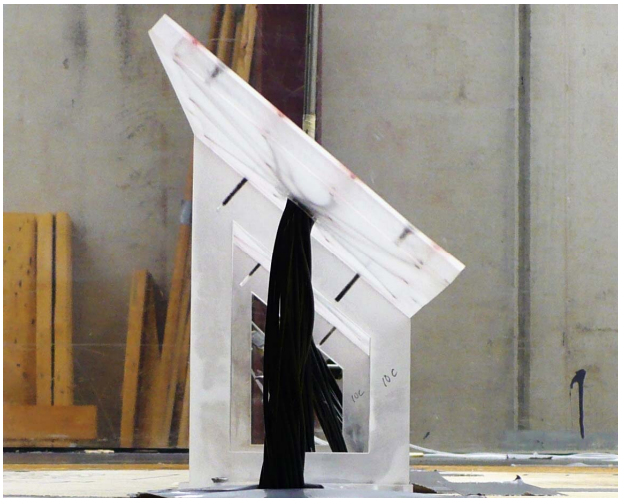
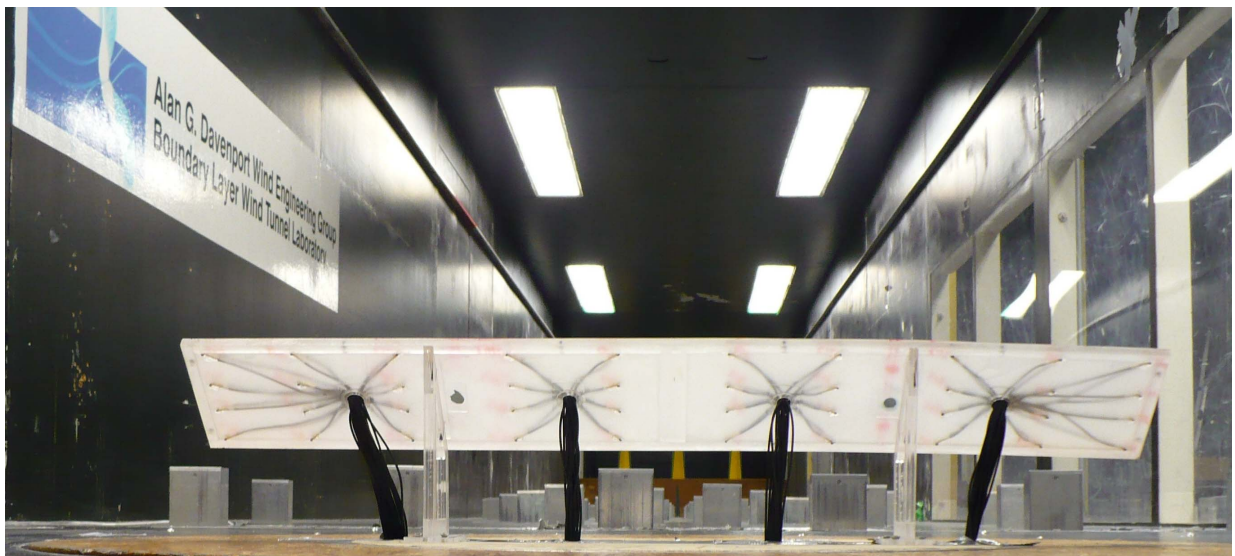


Fig. 2 Instrumented model-scale of a ground-mounted solar panel in the boundary layer test section. Four different configurations of the solar panels were used: (a) tilt angle  $\alpha$  of  $25^\circ$  and leg height (H) of 24 inches (25degH24), (b) tilt angle of  $25^\circ$  and leg height of 32 inches (25degH32), (c) tilt angle of  $40^\circ$  and leg height of 24 inches (40degH24), and (d) tilt angle of  $40^\circ$  and leg height of 32 inches (40degH32). 1 inch = 0.0254 m.

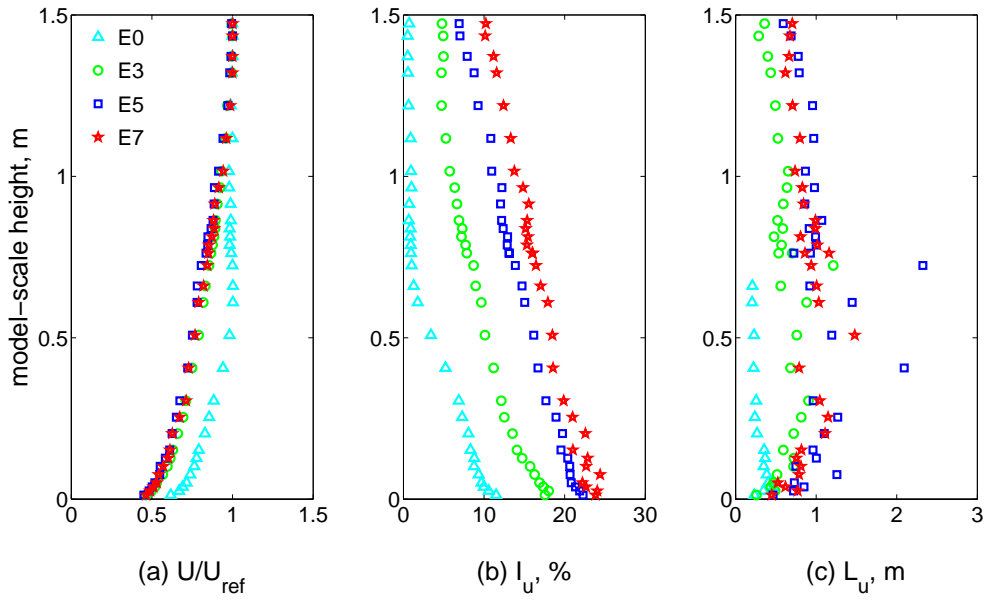


Fig. 3 Wind tunnel velocity profiles: (a) mean wind speed profile, (b) turbulence intensity profile and (c) integral length scale profile.  $U$  is the along-wind velocity component.

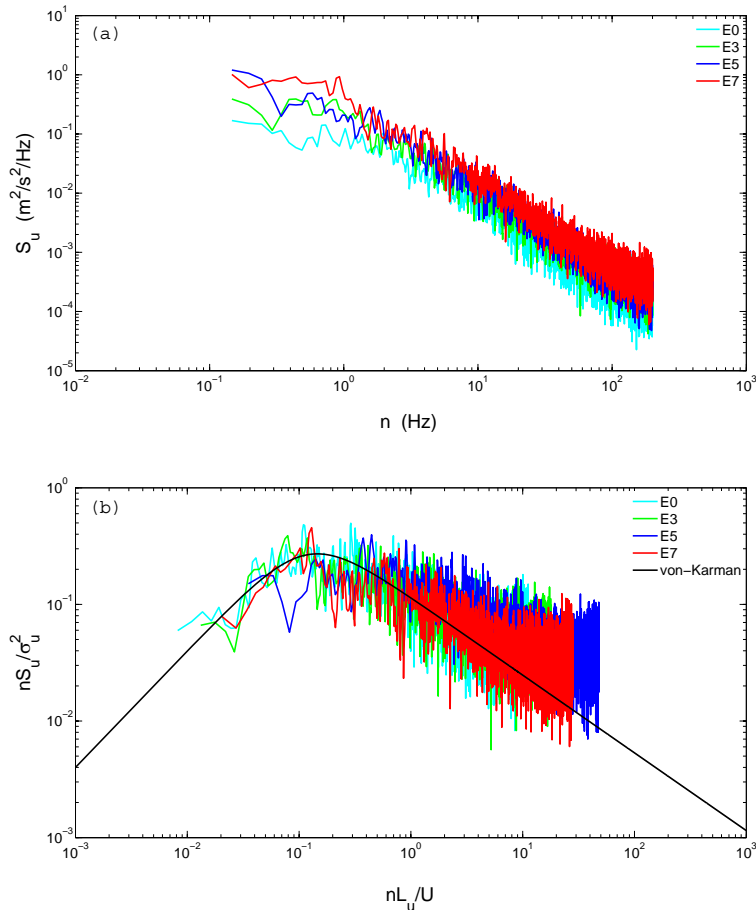


Fig. 4 Wind spectra of the along-wind velocity component ( $U$ ): (a) non-dimensional spectra and (b) normalized spectra along with the von-Karman spectra.

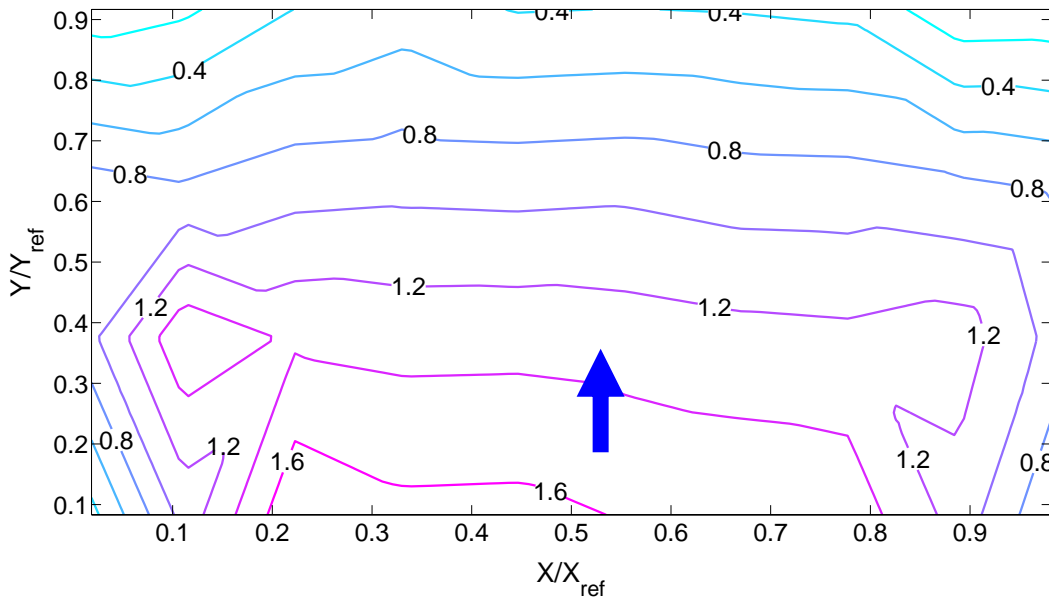


Fig. 5 Mean net pressure coefficient's ( $C_{p_{mean}}$ ) distribution over a solar panel module with scale 1:20; the arrow shows wind direction.  $Y_{ref}$  and  $X_{ref}$  are width and length of the panel, respectively.

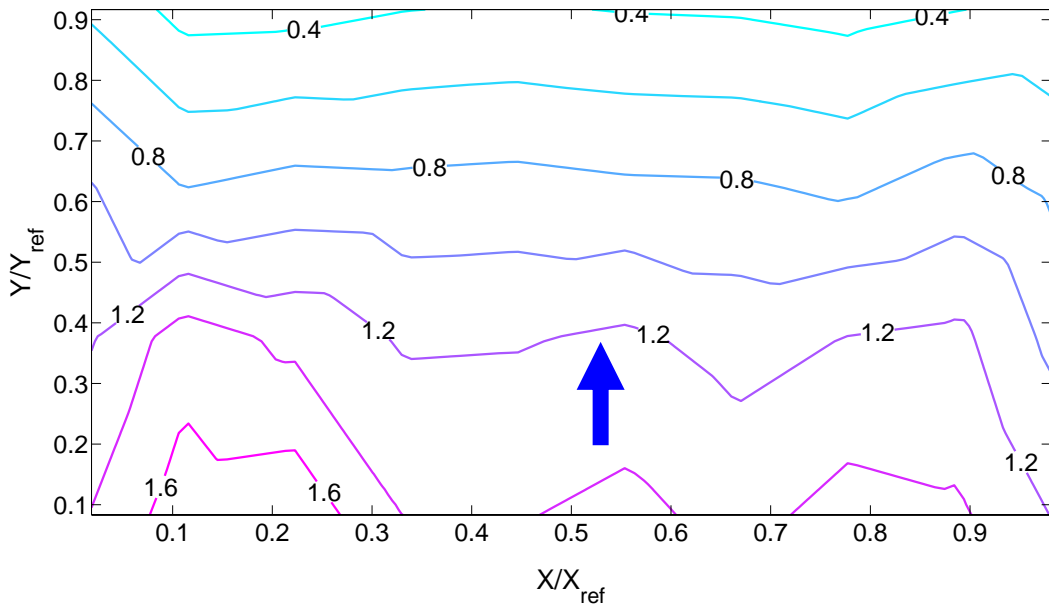


Fig. 6 Mean net pressure coefficient's ( $C_{p_{mean}}$ ) distribution over a solar panel module with scale 1:10; the arrow shows wind direction.  $Y_{ref}$  and  $X_{ref}$  are width and length of the panel, respectively.

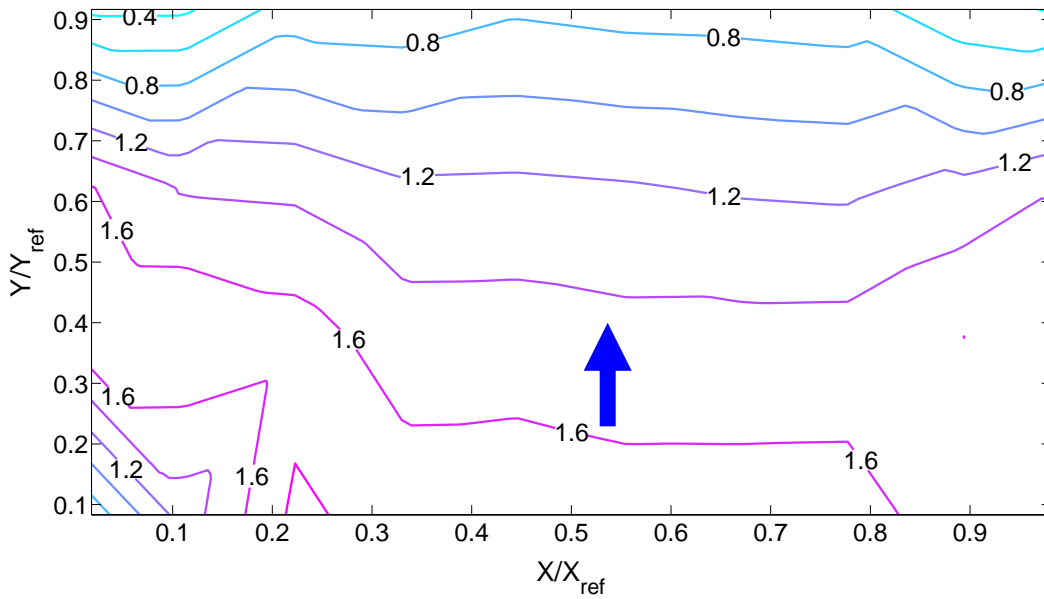


Fig. 7 Root mean square net pressure coefficient's ( $C_{p_{mean}}$ ) distribution over a solar panel module with scale 1:20; the arrow shows wind direction.  $Y_{ref}$  and  $X_{ref}$  are width and length of the panel, respectively.

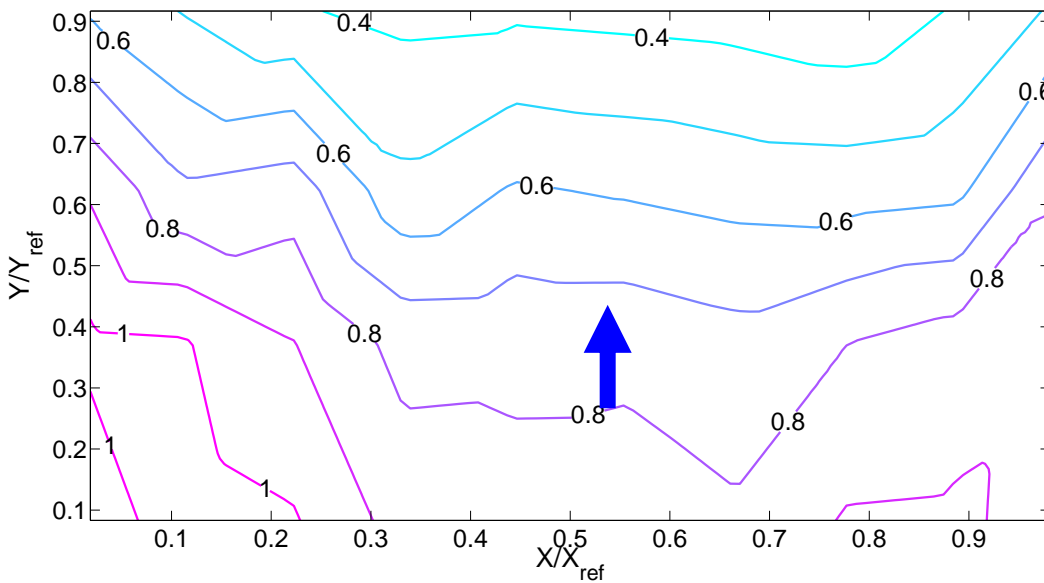


Fig. 8 Root mean square net pressure coefficient's ( $C_{p_{mean}}$ ) distribution over a solar panel module with scale 1:10; the arrow shows wind direction.  $Y_{ref}$  and  $X_{ref}$  are width and length of the panel, respectively.

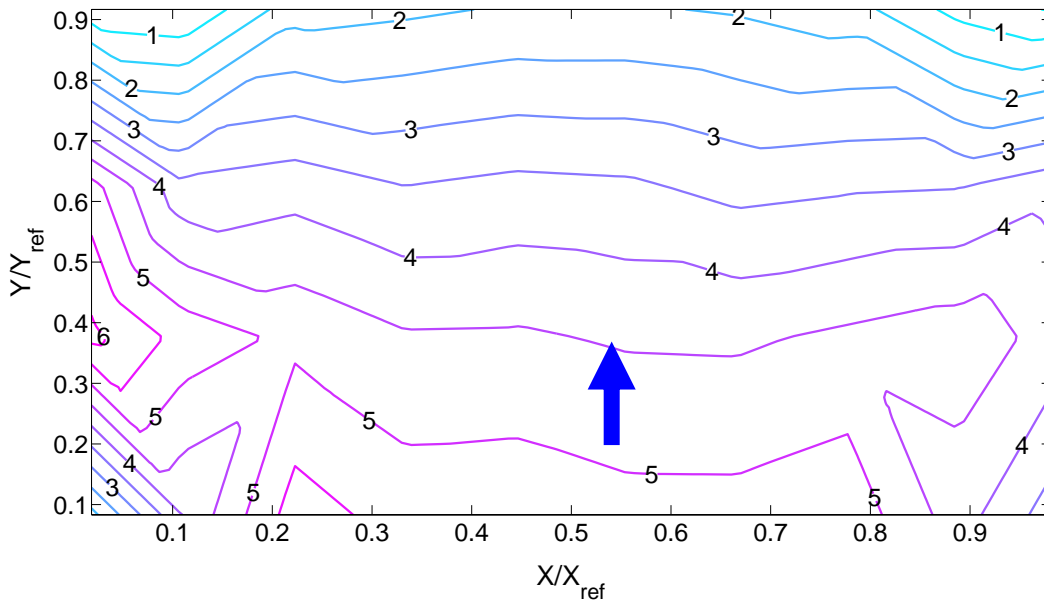


Fig. 9 Maximum net pressure coefficient's ( $C_{p_{mean}}$ ) distribution over a solar panel module with scale 1:20; the arrow shows wind direction.  $Y_{ref}$  and  $X_{ref}$  are width and length of the panel, respectively.

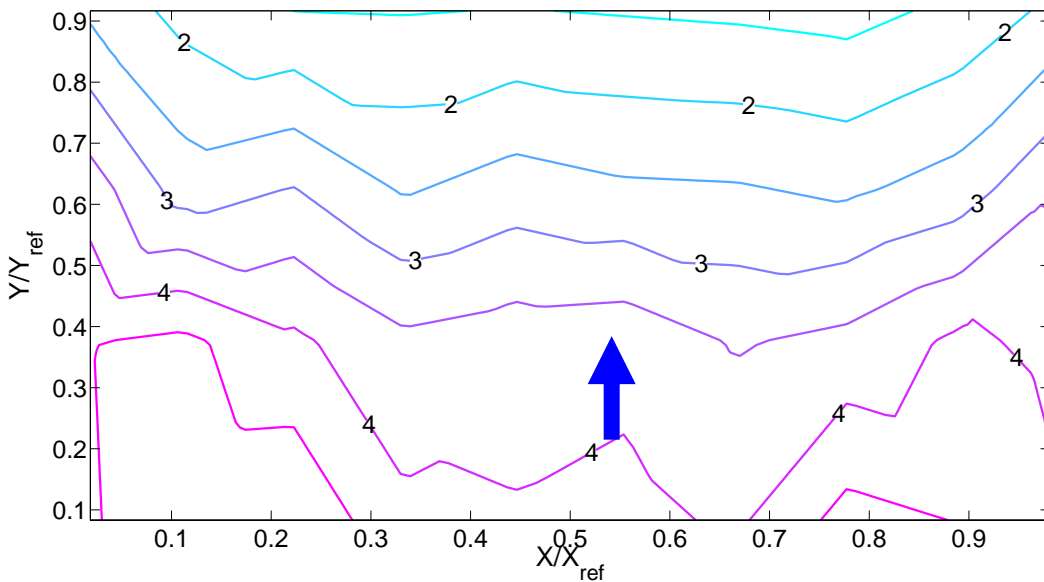


Fig. 10 Maximum net pressure coefficient's ( $C_{p_{mean}}$ ) distribution over a solar panel module with scale 1:10; the arrow shows wind direction.  $Y_{ref}$  and  $X_{ref}$  are width and length of the panel, respectively.

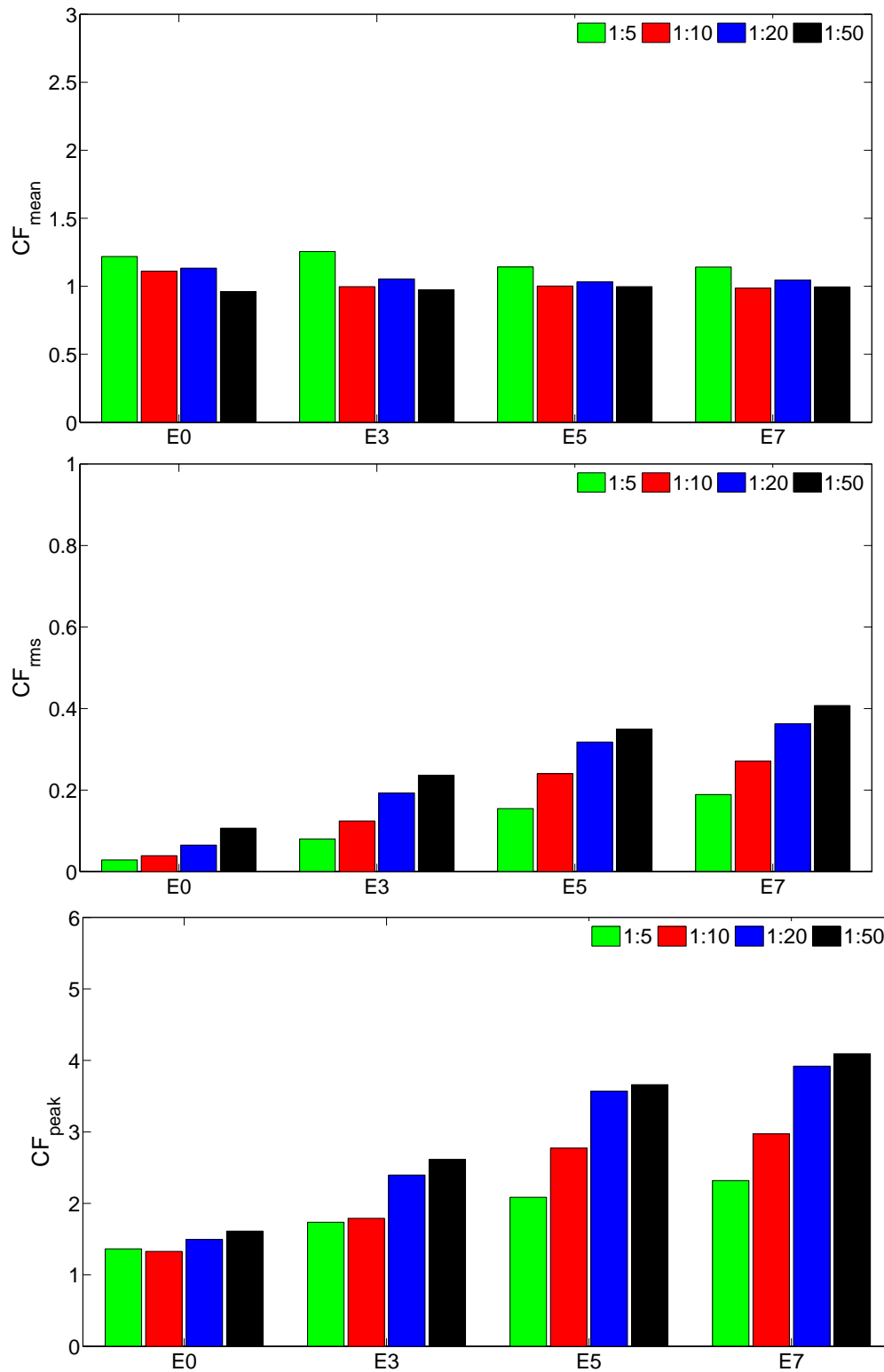


Fig. 11 Mean, root mean square and peak normal force coefficients for solar panel modules with tilt angle  $\alpha$  of  $25^\circ$  and leg height (H) of 24 inches (25degH24, see Fig. 2 ) under different wind exposures.



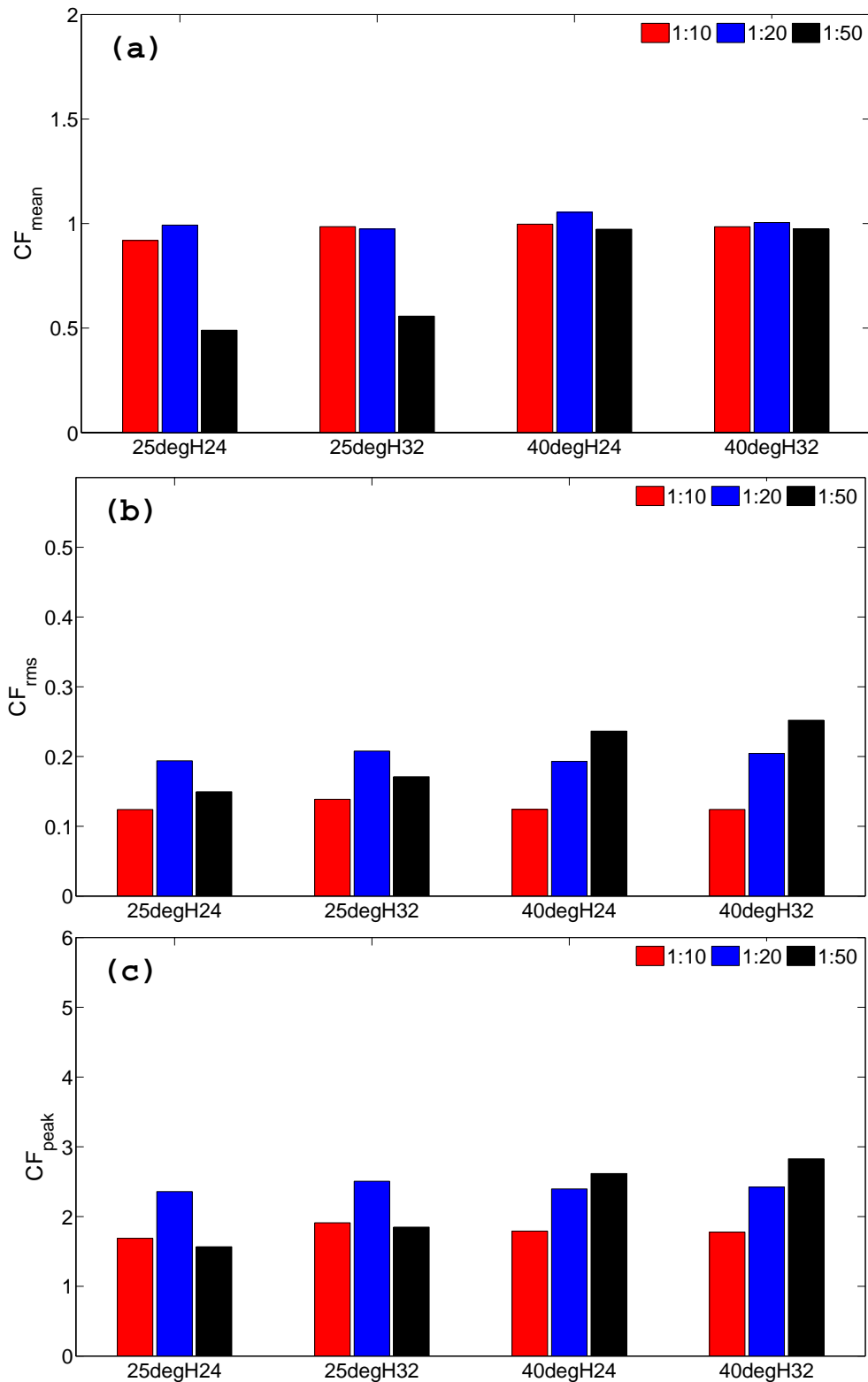


Fig. 12 Mean, root mean square and peak normal force coefficients for solar panel modules (total of four configurations were used: 25degH24, 25degH32, 40degH24 and 40degH32 as explained in Fig. 2 ) under wind exposure “E3.”